

Baryonic contributions to the dilepton spectra in relativistic heavy ion collisions

M. Bleicher*, A. K. Dutt-mazumder†, C. Gale†, C. M. Ko‡ and V. Koch*

* *Nuclear Science Division, Lawrence Berkeley National Laboratory
Berkeley, CA 94720, USA*

† *Physics Department, McGill University, Montreal, Quebec H3A 2T8, Canada*

‡ *Cyclotron Institute and Physics Department, Texas A&M University
College Station, TX 77843, USA*

We investigate the baryonic contributions to the dilepton yield in high energy heavy ion collisions within the context of a transport model. The relative contribution of the baryonic and mesonic sources are examined. It is observed that most dominant among the baryonic channels is the decay of $N^*(1520)$ and mostly confined in the region below the ρ peak. In a transport theory implementation we find the baryonic contribution to the lepton pair yield to be small.

I. INTRODUCTION

One of the main goals of relativistic heavy ion physics is to explore the possibility of studying strongly interacting matter in a highly exotic form: the quark gluon plasma. In this context the production of dileptons in high energy heavy ion collisions has received particular attention in recent years. This interest is due to the fact that dileptons, once produced, essentially decouple from the strongly interacting system and will reach the detectors mostly unscathed. Hence the dileptons serve as a promising probe, as their production rate is biased towards regions of high densities and high temperatures. Information on those is only available indirectly if one is limited to hadronic observables.

It is possible to roughly separate the dilepton invariant mass region in three parts: the “soft” dileptons essentially lie below the ϕ peak and the “hard” dileptons lie beyond the J/ψ . The region in-between has been coined the “intermediate mass region”. It is important to realize that different physics can be at work in those different regimes, mainly reflecting the different epochs of the relativistic nuclear collisions. For example, the hard dileptons will receive an important contribution from the Drell-Yan process which will happen in the first instants of the interaction. In this work, we shall restrict our attention to the soft part. This region is of interest as it has been the focus of detailed recent experimental measurements. Those were done by the HELIOS/3 [1] and CERES [2] collaborations, respectively. Those heavy ion experiments have reported an excess of lepton pairs over measurements involving proton-nucleus collisions. This has stimulated a great deal of theoretical activity [3–5] which has been summarized recently [6,7].

The theoretical interpretation of the dilepton excess has mostly concentrated on possible in-medium effects. One school of thought attributes the low mass abundance to a dropping vector meson mass, precursor of a chiral symmetry restoration in the dense medium [8]. Another evaluates the in-medium ρ spectral function and finds it considerably broadened (its peak value is not shifted appreciably), owing mainly to the coupling of the ρ with baryonic resonances [4]. But, to be precise, the effect is distributed over several channels [7]. However, the current experimental data are also consistent with a scenario without in-medium modifications [9,10]. Certainly, data with better statistics and an improved mass resolution are needed to extract any possible in-medium effects as well as to distinguish between the different in-medium modifications.

Several issues deserve further investigations in this matter. The dilepton calculations based on in-medium spectral functions receive a substantial contribution from the baryonic sector [4]. This feature is at first view puzzling, since the baryons are a minor component of the hadron population at CERN energies [11]. A rough estimate of the contribution of baryons to the dilepton channel had been provided in [5], and turned out to be about a factor of two below the contribution of the ω -Dalitz decay. With this in mind, we have set out to explicitly investigate the role of baryons in dilepton production in relativistic nuclear collisions. Our paper is organized as follows: we first explicitly examine the role of the $N^*(1520)$ resonance, which will turn out to be the largest baryon dilepton channel. We also examine a few subtleties associated with its off-shell behaviour and its coupling to electromagnetic radiation. We then compare rate calculations with each other in order to get a feeling for the magnitude of the different contributions in a somewhat idealized thermal environment. We then model the dynamics of the full nuclear collision in the UrQMD approach [12]. The transport model will cover aspects that are related to the possible importance of pre-equilibrium dynamics, while insuring a proper reproduction of the hadronic observables. It is important here to insist on the following: throughout this work the effective spectral function of the vector mesons are the vacuum ones, *i.e.* we will work with

an unmodified pion form-factor. Of course the spectral function associated with the electromagnetic current-current correlator will receive contribution from the medium, such as the Dalitz decays of mesons and baryons inside the fireball [10]. Therefore in this language the low mass lepton pairs come from hadron reactions and Dalitz decays. While formally the lepton pair production process can be linked to the imaginary part of the vector meson self-energy [13], its connection to Dalitz decay is clear [14]. Bear in mind that a consistent transport treatment of in-medium spectral functions is a topic that still requires development. In keeping with our focus on the role of baryons we then formulate a prediction for the dilepton spectra measured in recent low-energy runs of the CERN SPS. We finally conclude.

II. BARYONIC INTERACTIONS

Since one of the main issues we wish to address in this work is the role played by baryons in the production of low mass lepton pairs, this section first deals with technical issues that arise in such calculations. The baryons will mostly manifest themselves through their radiative decay channel into a dilepton. To fix the ideas, we explicitly consider the case of spin 3/2 baryon resonances which will turn out to be the most important contribution in any case. The channel we are considering is thus $R \rightarrow N e^+ e^-$, where R denotes the baryon resonance. The interaction Lagrangian is [15]

$$\mathcal{L}_{RN\gamma} = \frac{ieg_1}{2M} \bar{\psi}_R^\mu \Theta(z_1)_{\mu\nu} \gamma_\lambda \Gamma T_3 \psi_N F^{\nu\lambda} - \frac{eg_2}{4M^2} \bar{\psi}_R^\alpha \Theta_{\alpha\mu}(z_2) T_3 \Gamma \partial_\nu \psi_N F^{\nu\mu} + h.c. , \quad (2.1)$$

where $\Theta_{\mu\nu}(z) = g_{\mu\nu} - 1/2(1 + 2z)\gamma_\mu\gamma_\nu$. Γ is either 1 or γ_5 depending upon the parity of the resonances and T is a $3/2 \rightarrow 1/2$ isospin transition operator or a 2×2 Pauli matrix, depending on the isospin of the resonance. Ψ_R^μ and ψ correspond to Rarita-Schwinger and nucleon spinors respectively, $F^{\mu\nu}$ is the electromagnetic field tensor, and M is the nucleon mass. The influence of the off-shell parameter z is seen in calculations of electromagnetic transitions of nucleon resonances into different multipolarities [15]. It should be mentioned here that when the spin 3/2 particle is on-shell the results are independent of parameter z . Explicit calculation shows that the Rarita-Schwinger projection operator

$$\Delta_{\mu\nu}(q) = (\not{q} + M_R)(-g_{\mu\nu} + \frac{2}{3} \frac{q_\mu q_\nu}{M_R^2} + \frac{1}{3} \gamma_\mu \gamma_\nu - \frac{1}{3} \frac{q_\mu \gamma_\nu - q_\nu \gamma_\mu}{M_R}) \quad (2.2)$$

which appears in the squared matrix element for the decay of the 3/2 resonance contracted with z -dependent vertex terms γ_μ vanishes for on-shell particles. In other words, only the first term of the $\Theta_{\mu\nu}(z)$ remains operative for vertex involving on-shell 3/2 resonances. The presence of the second term in the Lagrangian is important in order to keep the electric quadrupole (E2) and magnetic dipole (M1) transitions independent [15]. Quantitatively however, we find that the contributions from the second term to the dilepton yield are smaller than that from the first one by an order of magnitude.

Before going into more detailed discussions, we point out some differences between this work and some current popular approaches [4,16] that rely on a nonrelativistic (NR) reduction of

$$\mathcal{L} = \frac{f_{RN\rho}}{m_\rho} \bar{\Psi}_R^\mu \gamma^\nu T F_{\mu\nu} \psi_N \quad (2.3)$$

to calculate the ρ spectral function. To cast it into the form relevant for the NR case, one neglects the lower component of the Dirac spinor and upon simplification one obtains

$$\mathcal{L} = \frac{f_{RN\rho}}{m_\rho} \Psi_R^\dagger (S_k \rho_k \omega - \rho_0 S_k q_k) \psi_N \quad (2.4)$$

where S_k ($k = 1, 2, 3$) is the 3/2 spin transition operator [17], $\rho^\mu = (\rho_0, \rho_k)$ is the ρ meson field, and $q^\mu = (\omega, q_k)$ is its four momentum.

The approach represented by Eq. (2.1) enables a study of the influence of the off-shell parameter z . This is done later on. By setting $z = -1/2$ and $g_2 = 0$ and using the the Vector Meson Dominance model (VMD), Eq.(2.1) can be cast in the form of the Lagrangian of Eq. (2.3). We note that it is satisfying to have a context where the importance of relativistic effects can be appreciated quantitatively. Those are found to be of some importance in the lower invariant mass region, as we will see shortly.

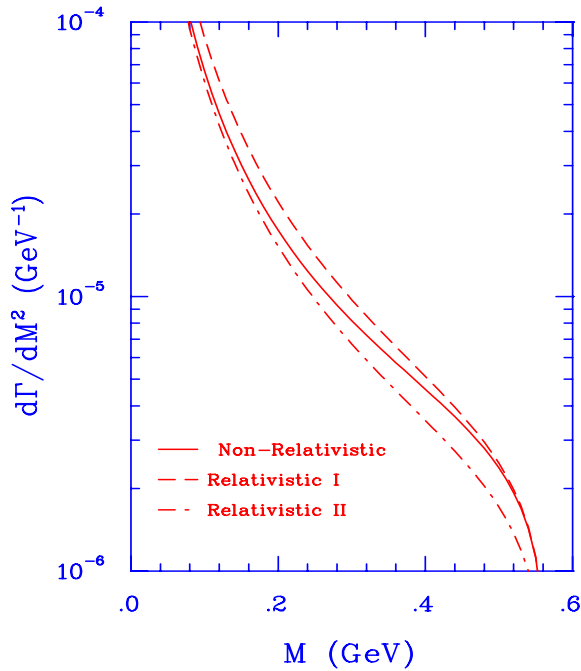


FIG. 1. Solid and dashed lines represent results obtained with the non-relativistic and relativistic versions of Eq. (2.3). The dashed-dotted line shows the result obtained with Eq. (2.1).

Let us consider the $N^*(1520)$ resonance. In the interaction Lagrangian of Eq. (2.1) we use parameters obtained in Ref. [18], where a fit to pion photoproduction multipoles was performed. To be quantitative, we take $g_1 = -1.839$, $g_2 = 0.018$, $z_1 = -0.092$ and $z_2 = -0.024$. There exists other parameter sets which yield comparable χ^2 as far as the photoproduction data is concerned, but in addition we will require sensible results for the calculation of radiative decay channels. The above quoted values of the parameter set yields the following widths: $\Gamma_{N^*(1520) \rightarrow N\gamma} = 0.78$ MeV and $\Gamma_{N^*(1520) \rightarrow N\rho} = 22.35$ MeV. The experimental values are 0.55 ± 0.1 MeV and 24.0 ± 6.0 MeV respectively. Using VMD with the nonrelativistic interaction Lagrangian Eq. (2.4) and fitting its only constant in order to reproduce $\Gamma_{N^* \rightarrow N\rho}$, one obtains $f_\rho = 5.5$ and $\Gamma_{N\gamma} = 0.88$ MeV. Using the same f_ρ in the relativistic Lagrangian, Eq. (2.3), produces $\Gamma_{N\gamma} = 1.13$ MeV and $\Gamma_{N\rho} = 30$ MeV.

Given a Lagrangian, the differential partial width into a lepton pair of invariant mass M is calculated by standard techniques [19]. We first investigate the effects of the different interactions. We fix the mass of the $N^*(1520)$ at its central value (*i.e.* at the peak of the vacuum spectral function). The results are shown in Fig. 1. The solid and dashed curves labeled Non-Relativistic and Relativistic I respectively correspond to the cases where the Lagrangian (2.3) and its NR reduction (2.4) have been used with the same coupling constant, $f_\rho = 5.5$. Comparing those two curves thus permits a direct assessment of relativistic effects. Those are found to be largest at the photon point and they become smaller at larger invariant masses, where the nucleon has a smaller momentum. The relativistic and NR treatments should then be in agreement at the larger invariant masses and this is indeed the case. The dashed-dotted curve (Relativistic II) represents the differential width obtained using Eq. (2.1). The difference between the two relativistic results appear to be a simple overall scaling. We have verified that this overall shift in fact corresponds to the ratio of the two radiative decay widths in the two models. We recall the versatility and the success of the relativistic approach represented by Lagrangian (2.1) in terms of its capability to reproduce pion photoproduction multipoles and decay widths into γN and ρN final states. However, the quantitative differences with a nonrelativistic treatment are overall not large. The relativistic approach can also lend itself to a study of off-shell effects (owing to its z -dependence): a topic towards which we now turn.

We have calculated $d\Gamma/dM^2$ for $N^*(1520) \rightarrow Ne^+e^-$ in three different ways. First using the on-shell mass (“On-Shell”, in Fig. 2), then integrating over the vacuum spectral function of this resonant state with (“Off-Shell I”), and without (“Off-Shell II”) the z -dependent interaction. This latter case was achieved by setting $z = -1/2$. It is clear that off-shell effects can arise not only from the mass distribution but also from the associated vertex containing the factor $\Theta_{\mu\nu}(z)$. A comparison of those three approaches is shown in Fig. 2. It is seen that off-shellness can cause differences of at most a few percent. Summarizing this section, one concludes that in this case off-shell effects are not numerically important and that relativistic effects are slightly larger. However, a nonrelativistic treatment remains a sensible approximation.

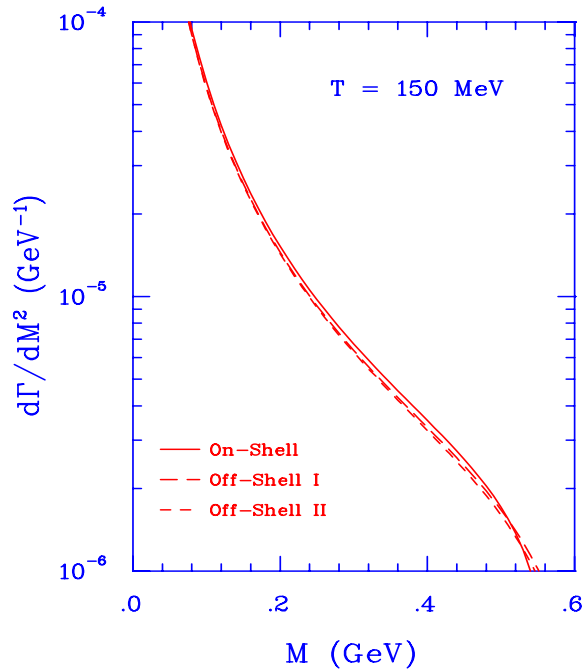


FIG. 2. The solid line shows results when $N^*(1520)$ is on-shell. The dashed-dotted and dotted curve depicts the results where the differential width has been integrated over $N^*(1520)$ spectral function with (Off-shell I) and with out off-shell interaction ($z = -1/2$) respectively (Off-shell II).

III. RATES

Before going into the transport calculation and thereby dealing with possible complications owing to the dynamics, we present thermal rate calculations of various lepton pair sources and compare them with each other. As discussed above, the relativistic effects are not large although not necessarily negligible. Note that the difference between the relativistic and non-relativistic results might become substantial, if evaluated in a different frame of reference [20]. However, in the present work we will employ the calculated decay within a transport model, where the widths are always evaluated in the rest frame of the resonance and then simply boosted to the appropriate matter frame. Thus, in this context using the non-relativistic expression for the widths is a good approximation. Using Eq. (2.4) and VMD, the differential partial width for the decay of baryonic resonance R_i into a nucleon and a lepton pair of invariant mass M can be written as [16]

$$\frac{d\Gamma_{R_i\rho}}{dM} = \left(\frac{f_{R_i N\rho}}{m_\rho} \right)^2 \frac{1}{\pi} S_\Gamma M \frac{m_N}{m_{R_i}} k_\rho A F_\rho(M) F(k_\rho^2), \quad (3.1)$$

where

$$\begin{aligned} A &= k_\rho^2 && \text{for } p\text{-wave} \\ &= 2k_\rho^2 + 3M^2 && \text{for } s\text{-wave}, \end{aligned} \quad (3.2)$$

and $F(k_\rho^2) = \Lambda^2 / (\Lambda^2 + k_\rho^2)$, with $\Lambda = 1.5$ GeV. In the above, $f_{R_i N\rho}$ is the coupling constant, S_Γ is the spin sum, and k_ρ is the momentum of the rho meson in the rest frame of the baryon resonance.

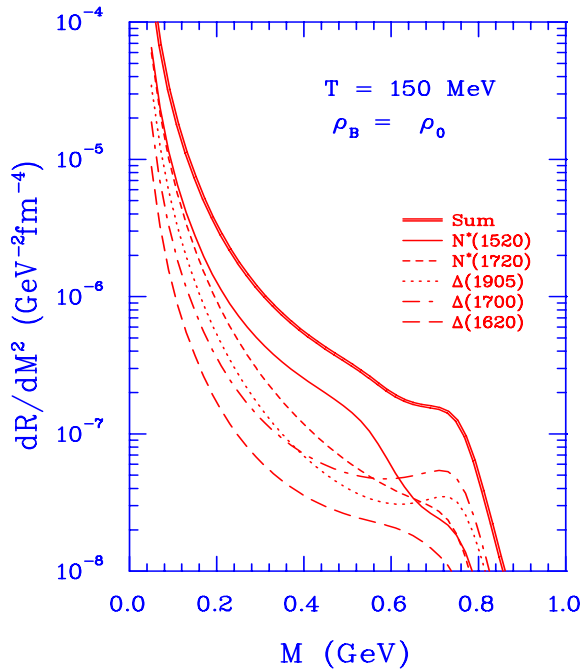


FIG. 3. Relative contributions of the baryonic resonances to the dilepton production rate and their sum.

We should note that the vector dominance coupling used here for the $N^*(1720)$ and $\Delta(1905)$ over-estimates the measured photon decay width [21]. Thus our results for the dilepton rates due to these resonances are in fact upper limits.

The ρ mass distribution is

$$F_\rho(M) = \frac{1}{\pi} \frac{m_\rho \Gamma_\rho(M)}{(M^2 - m_\rho^2)^2 + (m_\rho \Gamma_\rho(M))^2}. \quad (3.3)$$

One uses the differential decay width to derive the differential dilepton production rate. For a general process $a \rightarrow b + e^+e^-$, this is [19]

$$\frac{dR_{a \rightarrow b + e^+e^-}}{dM^2} = \frac{Nm_a}{(2\pi)^2} \frac{d\Gamma_{a \rightarrow b + e^+e^-}}{dM^2} \int_{m_a}^{\infty} dE_a p_a f_a(E_a) \int_{-1}^1 dx [1 + f_b(e_b)], \quad (3.4)$$

where $E_b = (E_a E_b^* + p_a p_b^* x)/m_a$ and $E_b^* = (m_a^2 + m_b^2 - M^2)/(2m_a)$ [19]. In the above we have assumed that a and b were fermions and thus the f 's are Fermi-Dirac distribution functions.

We first calculate and compare dilepton rates associated with the radiative decay of several hadronic resonances. The species we consider and the associated rates are shown in Fig. 3. We show representative results obtained at normal nuclear matter density. Adding to the sum of baryonic contributions the signal from $\pi - \pi$ annihilation and that from ω decay one obtains the net rates shown in Fig. 4.

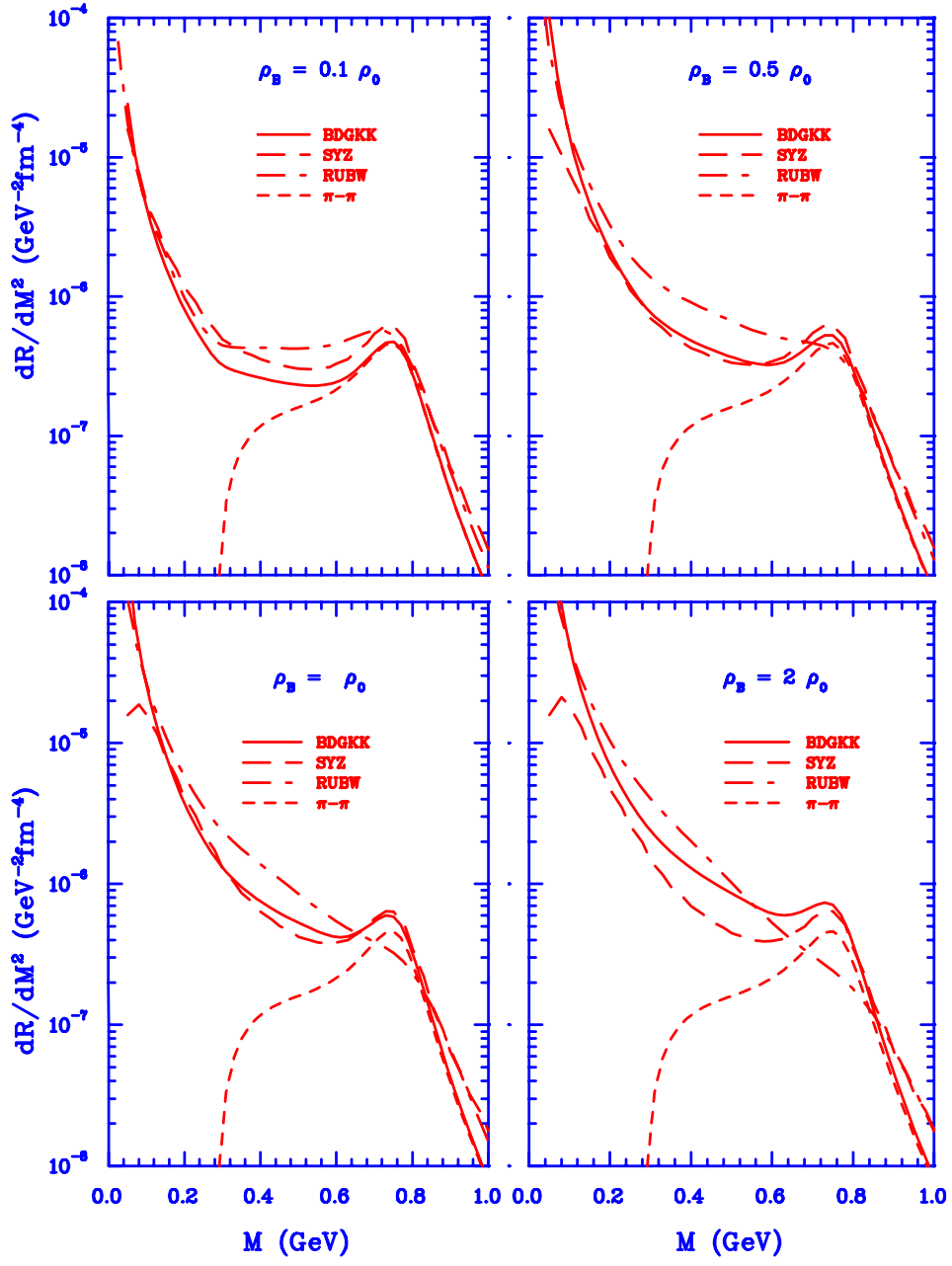


FIG. 4. Comparison of the rates obtained in this work with that of others at $T = 150$ MeV. The short-dashed curve corresponds to π - π annihilation only, and the full, long dashed and dashed dotted curves refer to the rates calculated here (DGKK), by SYZ and by RUBW respectively. See the main text for references.

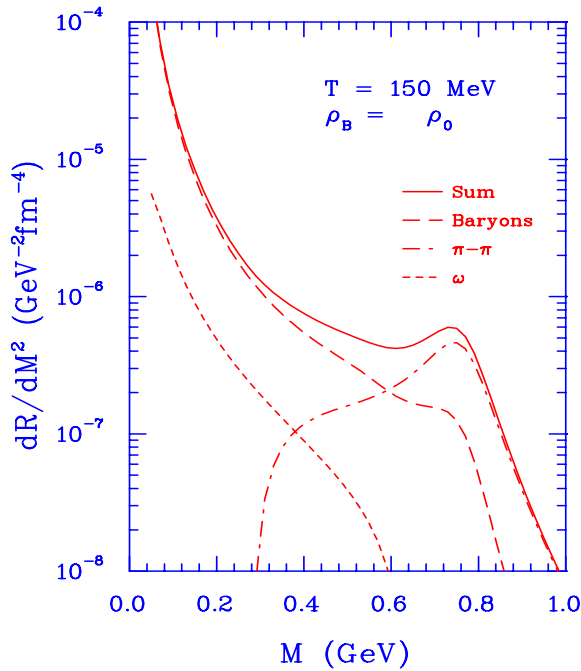


FIG. 5. The relative importance of mesonic and baryonic contribution to the dilepton rate is shown. The solid line corresponds to the total yield while the dashed line represents the sum over baryonic contributions. Dashed and dotted curves refer to the π - π annihilation and ω Dalitz decay, respectively.

The two mesonic sources we have considered are actually the largest ones in the invariant mass range we have chosen to consider. Also shown on Fig. 4 are the rates obtained by Steele, Yamagishi, and Zahed (SYZ) [22] and by Rapp, Urban, Buballa, and Wambach (RUBW) [23]. At very low baryonic densities, the three rates are quite close to each other. As the density grows our rates remain quite close to that obtained in the SYZ formalism. At the highest baryonic density we have considered, our results approximately lie in between those of SYZ and RUBW, for low invariant masses. A marked difference exists in the results of RUBW, that can be understood in terms of the spectral function re-summation technique leading to a suppression at the ρ peak [24]. To provide a reference point, the analysis of particle ratios for SPS-collision at 160 GeV per nucleon gives a chemical freeze-out temperature of about $T = 170$ MeV and a baryon density of about $\rho = \rho_0$ (see *e.g.* [25]). Finally, the relative importance of our mesonic and baryonic rates is shown in Fig. 5. The baryons dominate the low invariant mass region while the $\pi - \pi$ channel picks up near the ρ peak. Representative results at normal nuclear matter density are shown. The relative importance of mesons and baryons does not change considerably if one uses the chemical freeze-out temperature of 170 MeV. It is finally important to realize that the actual contribution from the ω Dalitz decay to the final measurements is much higher than it appears from Fig. 5: the dominant part is due to the decay of the final state ω 's.

IV. TRANSPORT CALCULATION

The nuclear dynamics and dilepton production is studied here within the framework of the Ultra-Relativistic Quantum Molecular Dynamics model, UrQMD [12]. In addition to earlier molecular dynamics models its collision term describes the production of all established meson and baryon resonances up to about 2 GeV with all corresponding isospin projections and antiparticle states.

In the present model, light meson formation at low energies is modeled by multi-step processes that proceed via intermediate heavy meson and baryon resonances and their subsequent decay [12]. The pole masses, decay widths and branching ratios of all resonances are taken from [26]. However, due to the experimental uncertainties a certain range of parameters might be used to obtain a consistent fit to cross section data. As an example, the production of ω mesons is described in the UrQMD model by the formation and the decay of the $N^*(1900)$ resonance. It decays in 35% of the cases into $N\pi$ and 55% into $N\omega$. In line with data at SIS energies (1 AGeV), the η production proceeds not only via $N^*(1535)$, but invokes also nucleon resonances with masses from 1650 MeV to 2080 MeV. A detailed description of the resonance formation cross sections and comparisons to data is give in Ref. [12]. For earlier works on dileptons within the same framework see *e.g.* [27].

Dilepton production is calculated in the following way. We consider two distinct classes of processes. First, direct decays of vector mesons, i.e. the ρ and ω mesons. Second, the Dalitz decay of mesons and baryons during the reaction, specifically the ω and a_1 meson as well as the $N^*(1520)$. The Dalitz decay of the pion and eta is treated at the end of the simulation according to Ref. [5]. By treating the direct decay of the ρ we implicitly also include the contribution from the pion annihilation channel (see *e.g.* [5]). In order to avoid double counting, we do not allow ρ mesons created via the decay of the $N^*(1520)$ or a_1 -meson to decay into dileptons, since we treat the Dalitz decay of these states explicitly. Since in UrQMD the ω -meson does not have a $\rho - \pi$ decay channel, there is no double counting in this channel. One should note at this point that treating the Dalitz decays as a two-step process via an intermediate ρ meson can lead to erroneous results in a transport description: in this case lepton pairs below the minimum mass of $m < 2m_\pi$ cannot be produced while this is of course kinematically allowed for a Dalitz decay.

In order to extract the dilepton yield from UrQMD, we extract for each of the aforementioned channels the lifetime and four-momentum. The properties of the individual hadrons are given by the collision dynamics. If a meson is produced in an elementary collision (may it be due to string fragmentation, meson or baryon resonance decay or annihilation) it gets a mass according to a Breit-Wigner distribution and a 4-momentum vector according to the kinematics of this single reaction. The meson is then assumed to travel on a straight line trajectory until it (i) decays or (ii) collides with another particle and its 4-momentum changes. Any change of the 4-momentum of the meson is considered as a destruction of the original meson and the creation of a new meson with new quantum numbers and a new 4-momentum. Thus for each hadron under consideration UrQMD provides a list of four-momenta q and lifetimes Δt , $\{\{q, \Delta t\}_i\}_h$, where the index h labels the hadron, and i labels the different four-momenta and time-intervals for which the hadrons exists during the course of the collision. The resulting dilepton spectrum is then obtained from

$$\frac{dN_{l+l^-}}{dM} = \sum_i \left(\Delta t_i \Gamma_{V \rightarrow l+l^-}(M) \delta \left(\sqrt{q_i^2} - M \right) \right)_{h=V} \quad (4.1)$$

for the the direct decay of vector-mesons. For the Dalitz decays, on the other hand we have

$$\frac{dN_{l+l^-}^{\text{Dalitz}}}{dM} = \sum_i \left(\Delta t_i \frac{d\Gamma(q_i^2)_{R \rightarrow l+l^- X}}{dM} \right). \quad (4.2)$$

If absorption is negligible, this approach is equivalent to the method of adding one dilepton (with appropriate normalization) at each decay vertex. However, this “shining” method gives better numerical statistics compared to a single decay of the vector meson. To get an upper limit on the possible dilepton radiation, particles are allowed to couple to the dilepton channel also during their formation time. If we insist that the particles shine only after their formation time is over, we have verified that the net rate is only reduced by $\approx 25\%$.

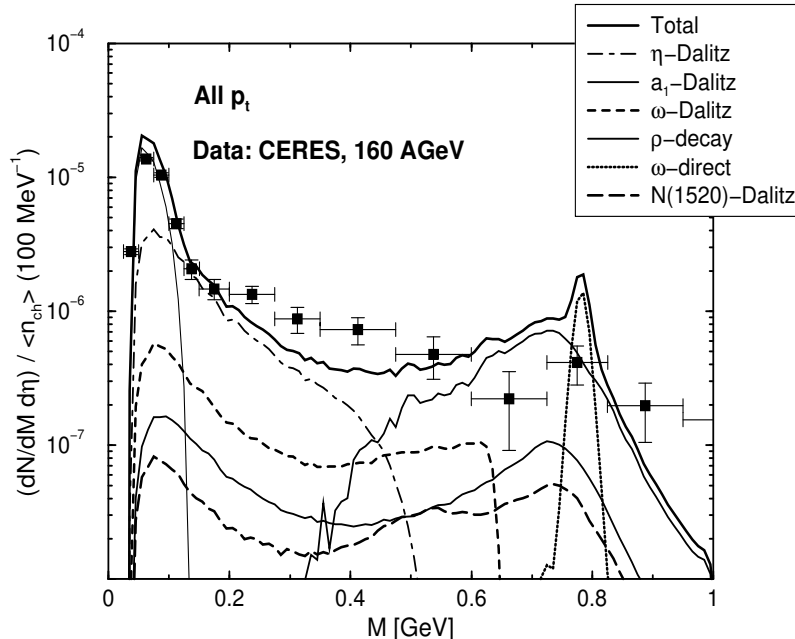


FIG. 6. Invariant mass spectrum for all pair momenta, for Au-Au collisions at 40 AGeV. Data are from [2] and are shown only to set a scale. See the text for details.

Since we are specifically concerned with the role of the baryons in the production of lepton pair, we present a set of predictions for recent CERN low-energy runs where baryon density effects should be larger than for the high energy runs. Those predictions appear in Figs. 6, 7 and 8.

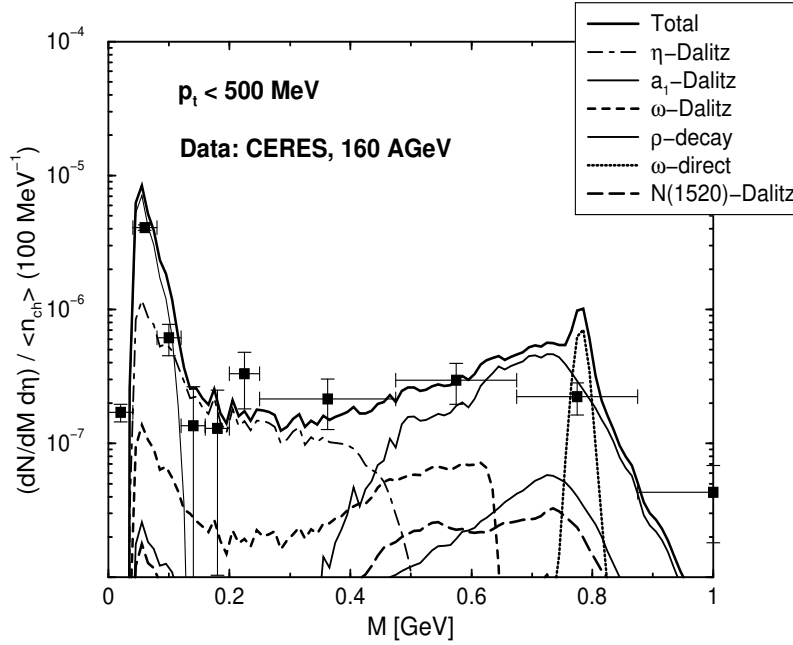


FIG. 7. Same caption as for Fig. 6, but only for low p_T lepton pairs.

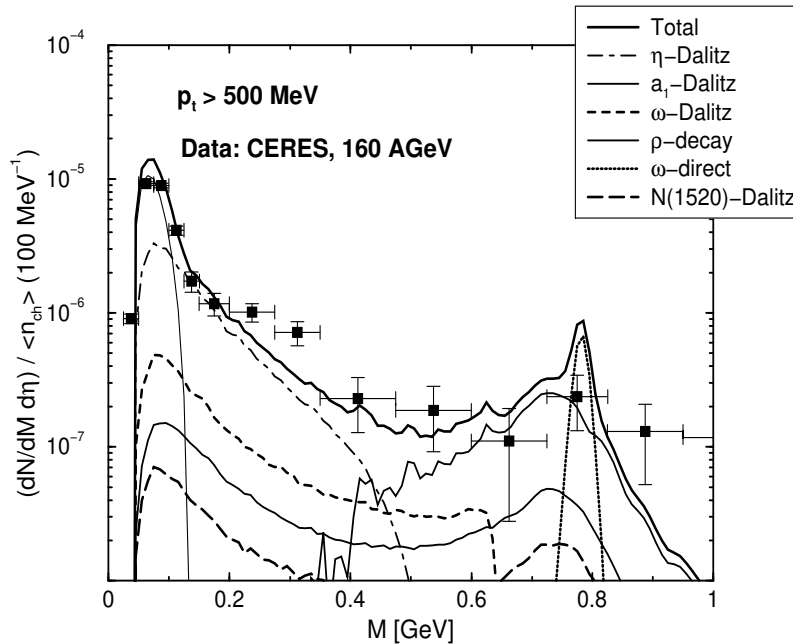


FIG. 8. Same caption as for Fig. 6, but for high p_T lepton pairs.

To provide a visual scale reference, we also show data by the CERES collaboration for 160 AGeV collisions [2]. Aside from the clearly visible ω -peak, we predict that there will be little difference between the “high-energy” (160 AGeV) and “low-energy” (40 AGeV) dilepton invariant mass spectra. At an invariant mass of 400 MeV, the 160 AGeV

calculation is 20% higher (including the CERES normalization) than the 40 AGeV one [28]. Here, we have worked with a mass resolution of $\Delta M/M = 1\%$. If this resolution can be achieved in experiment, the omega-peak should be clearly visible, providing a strong constraint for presently available model calculations. Furthermore, we find that the contribution of the $N^*(1520)$ -Dalitz (thick dashed curve) is very small, even at these low bombarding energy. We finally note, that a calculation based on the model of [5] with the addition of the $N^*(1520)$ channel and constrained by the final state hadronic spectra as predicted by the RQMD model for a 40 AGeV collision, gives virtually the same results. This model also is in fair agreement with the dilepton spectra measured in the higher energy collisions [10].

V. CONCLUSION

We see that our transport results lead to a very small baryonic contribution to the net dilepton yield for the recently done low energy heavy ion runs of the CERN SPS. This is to be contrasted with the baryon influence on the net rate, as shown in Fig. 5. The reason for this difference is two-fold. First, the baryonic contribution are severely cut down by the CERES acceptance which we apply to our transport results in Figs. 6 and 7. Second, the baryon content of the central rapidity region is smaller than its mesonic content, owing to the dynamics of the stopping power systematics and of the phase space for particle creation. The small baryon contributions obtained here can be compared with similar results obtained with a hydrodynamic model [29]. Therefore it really does appear that the ideal test to pin down the relevant dilepton production scenario would involve a low energy run. A high resolution measurement at the positions of the vector meson vacuum masses would highlight the high baryon density. In such an environment the collective behaviour of the many-body calculations leads to a suppression of the vector meson peak [24]. In this context we have generated a set of predictions and the corresponding dilepton results of the CERN low energy runs are eagerly awaited. We are also looking forward to HADES measurements at the GSI [30] where it has been shown that the dilepton contribution from $N^*(1520)$ Dalitz decay is most important in the invariant mass region $0.35 < M < 0.75$ GeV/ c^2 [31].

ACKNOWLEDGMENTS

CG, CMK, and VK wish to acknowledge the hospitality of the Theory Institute of the University of Giessen, where this work was started. We also would like to thank P. Huovinen for furnishing the SYZ and RUBW rates used in Fig. 4. The work of CG and AKDM is supported in part by the Natural Sciences and Engineering Research Council of Canada and in part the Fonds FCAR of the Québec Government. The work of CMK is supported by the National Science Foundation under Grant No. PHY-9870038, the Welch Foundation under Grant No. A-1358, the Texas Advanced Research Program under Grants No. FY97-010366-0068 and FY99-010366-0081, and the Alexander von Humboldt Foundation. VK and MB are supported by the Director, Office of Energy Research, division of Nuclear Physics of the Office of High Energy and Nuclear Physics of the U.S. Department of Energy under Contract No. DE-AC03-76SF00098. MB is supported by a Feodor-Lynen fellowship of the Alexander von Humboldt Foundation.

-
- [1] M. Masera et al., Nucl. Phys. **A590**, 93c (1995).
 - [2] B. Lenkeit, in *Proceedings of INPC 98*, Paris Aug. 24-28, 1998, Nucl. Phys. A to be published, and references therein.
 - [3] G. Q. Li, C. M. Ko, and G. E. Brown, Phys. Rev. Lett. **75**, 4007 (1995); D. K. Srivastava, B. Sinha, and C. Gale, Phys. Rev. C **53**, R567 (1996); G. Q. Li, C. M. Ko, and G. E. Brown, Nucl. Phys. **A606**, 568 (1996); **A611**, 539 (1996); W. Cassing, W. Ehehalt, and C. M. Ko, Phys. Lett. **B377**, 5 (1996).
 - [4] R. Rapp, G. Chanfray, and J. Wambach, Phys. Rev. Lett. **76**, 368 (1996); Nucl. Phys. **A617** 472 (1997).
 - [5] V. Koch and C. Song, Phys. Rev. C **54** 1903(1996).
 - [6] C. M. Ko, V. Koch, and G. Q. Li, Ann. Rev. Nucl. Sci. **47**, 505 (1997).
 - [7] R. Rapp and J. Wambach, submitted to Adv. Nucl. Phys.; hep-ph/9909229.
 - [8] G.E. Brown and Mannque Rho, Phys. Rep. **269**, 333 (1996).
 - [9] V. Koch, Proc. of 37th Intl. Winter Meeting on Nuclear Physics, Bormio, Italy, 25-29 Jan 1999; nucl-th/9903008.
 - [10] V. Koch et al., Proc. 28th Intl. Workshop on Gross Properties of Nuclei and Nuclear Excitation: Hadrons in Dense Matter (Hirscheegg 2000), Hirscheegg, Austria, 16-22 Jan 2000; nucl-th/0002044.
 - [11] J. Stachel, Nucl. Phys. **A610**, 509c (1996).

- [12] M. Bleicher et al., J. Phys. **G** 25, 1859 (1999); S. Bass *et al.*, Prog. Part. Nucl. Phys. **41**, 225 (1998).
- [13] Charles Gale and Joseph I. Kapusta, Nucl. Phys. **B357**, 65 (1991).
- [14] H. A. Weldon, Phys. Rev. D **28**, 2007 (1983).
- [15] M. Benmerrouche and Nimai C. Mukhopadhyay, Phys. Rev. D **51**, 3237 (1995).
- [16] W. Peters, M. Post, H. Lenske, S. Leupold, and U. Mosel, Nucl. Phys. **A632** 109 (1998).
- [17] Pions and Nuclei, T. Ericson and W. Weise, Oxford University Press, 1988.
- [18] T. Feuster and U. Mosel, Nucl. Phys. **A612**, 375(1997).
- [19] C. Gale and P. Lichard, Phys. Rev. D **49**, 3338 (1994).
- [20] M. Post, S. Leupold, and U. Mosel, to be published.
- [21] B. Friman and H.J. Pirner, Nucl. Phys. **A617** 496 (1997)
- [22] J. V. Steele, H. Yamagishi, and I. Zahed, Phys. Lett. **B384**, 255 (1997); Phys. Rev. D **56**, 5605 (1997).
- [23] R. Rapp, M. Urban, M. Buballa, and J. Wambach, Phys. Lett. B **417**, 1 (1998).
- [24] R. Rapp and C. Gale, Phys. Rev. C **60**, 024903 (1999).
- [25] P. Braun-Munzinger, I. Heppe, and J. Stachel Phys.Lett. **B465**, 15 (1999).
- [26] Particle data group, Phys. Rev. D **54**, 1 (1996).
- [27] C. Ernst *et al.*, Phys. Rev. C **58**, 447 (1998); nucl-th/9907118.
- [28] D. Dietrich *et al.*, in preparation.
- [29] P. Huovinen and M. Prakash, Phys. Lett **B450**, 15 (1999).
- [30] J. Friese *et al.*, Prog. Part. Nucl. Phys. **42**, 235 (1999).
- [31] E. L. Bratkovskaya and C. M. Ko, Phys. Lett. **B445**, 265 (1999).